

Anomalous Surface Compositions of Stoichiometric Mixed Oxide Compounds**

Sergiy V. Merzlikin, Nikolay N. Tolkachev, Laura E. Briand, Thomas Strunskus, Christof Wöll, Israel E. Wachs, and Wolfgang Grünert*

Surface-oxide films are present in many types of oxide-containing materials, such as grain boundaries in ceramics,^[1] interfaces in ceramic-ceramic^[2] and metal-oxide systems,^[3] and affect their materials and transport properties. In heterogeneous catalysis, the properties of the outermost surface layer are of prime importance because they control the catalytic performance.

Although bulk mixed-metal oxide catalysts are widely used in industrial selective oxidation processes,^[4,5] not much is

known about their outermost surface composition. Models based on surfaces derived from a truncation of the bulk structure have dominated discussion on catalytic reaction mechanisms and active sites (reviewed, for example, in Ref. [6]). This view has been questioned by several recent studies reporting the surface enrichment and depletion phenomena in solid-oxide solutions (e.g., $\text{Co}_x\text{Ni}_{1-x}\text{O}^{[7]}$), the identification of TiO_2 -rich overlayers on reconstructed $\text{SrTiO}_3(001)$ model surfaces,^[8] and evidence for the formation of amorphous oxide overlayers in which there is surface enrichment of one of the components under selective oxidation reaction conditions.^[9,10] However, the development of realistic concepts on reactant activation, surface reaction mechanisms, and the design of advanced catalytic materials are still hampered by the lack of detailed knowledge of the surface composition and structure of bulk mixed-metal oxides.

For such studies, X-ray photoelectron spectroscopy (XPS) with laboratory sources is of limited value because its average sampling depth of 1–3 nm results in a signal where the outermost surface layer only contributes on the order of 30%. Synchrotron radiation allows for increasing the surface sensitivity of XPS by decreasing excitation and, hence, photoelectron kinetic energies. Exclusive information on the outermost surface layer, however, is only given by low-energy ion scattering (LEIS) because ions penetrating below the surface become largely neutralized.^[11]

The surfaces of stoichiometric bulk mixed-metal molybdates and vanadates have also been characterized through their interactions with probe molecules, for example, CH_3OH ,^[12–15] which allows CH_3O^* and intact CH_3OH^* intermediates on different surface cations to be discriminated by IR spectroscopy. For such materials, combined methanol chemisorption and oxidation kinetic studies suggested a strong surface enrichment of MoO_x or VO_x .^[12,14,15] In methanol oxidation studies, similar catalytic turnover frequencies were found over bulk mixed-metal oxides and related supported metal oxides (e.g., $\text{Fe}_2(\text{MoO}_4)_3$ and $\text{MoO}_3/\text{Fe}_2\text{O}_3$), which supports the idea of surface MoO_x enrichment of the bulk phases.^[16–19] These observations, however, are qualitative as exposed metal oxide ions of low catalytic activity would not be detected by the test reaction. Thus, we have undertaken a study of the outermost surface compositions of such compounds by LEIS and excitation-energy resolved XPS (ERXPS). The LEIS was applied in sputter series taking advantage of its destructive character, the ERXPS is a version utilizing information from different sampling depths.^[20]

LEIS sputter series from stoichiometric bulk mixed oxides and related supported metal oxides are given in Figure 1 and

[*] Dr. S. V. Merzlikin,^[†] Prof. Dr. W. Grünert
 Lehrstuhl für Technische Chemie, Ruhr-Universität Bochum
 Postfach 102148, 44780 Bochum (Germany)
 Fax: (+49) 234-32-14115

E-mail: w.gruenert@techem.rub.de
 Homepage: <http://www.techem.rub.de>

Dr. N. N. Tolkachev,^[#]
 N. D. Zelinsky Institute of Organic Chemistry
 Russian Academy of Sciences, Moscow (Russia)

Dr. L. E. Briand
 Centro de Investigación y Desarrollo en Ciencias Aplicadas
 UNLP, CONICET, Buenos Aires (Argentina)

Dr. T. Strunskus,^[§] Prof. Dr. C. Wöll^[††]
 Lehrstuhl Physikalische Chemie I
 Ruhr-Universität Bochum (Germany)

Prof. I. E. Wachs
 Operando Molecular Spectroscopy and Catalysis Laboratory
 Department of Chemical Engineering, Lehigh University
 Bethlehem, PA 18015 (USA)

[†] Present address: Max-Planck Institute of Iron Research
 Düsseldorf (Germany)

[††] Present address: KIT, Institut für funktionelle Grenzflächen
 Karlsruhe (Germany)

[§] Present address: Christian-Albrechts-Universität Kiel (Germany)

[#] Present address: Rosnano Inc.
 Nametkina Street, 12A, 117420 Moscow (Russia)

[**] Financial support from the German Science Foundation (grant no. Gr 1447/9) is gratefully acknowledged. We also thank the Federal Ministry of Education and Research for the supporting travel grants (reg. no. 05 ES3XBA/5), the staff of BESSY II for continuous support, Dr. O. Shekhah for participating in the synchrotron measurements, and Dr. O. P. Tkachenko for participating in the LEIS measurements. I.E.W. acknowledges the support of Department of Energy (DOE)-Basic Energy Sciences (grant DEF-G02-93ER14350) for financial support. L.E.B. acknowledges the CONICET (USA–Argentina) collaboration (res. no. 0060) and Agencia Nacional de Promoción Científica (project PICTRedes 729/06). The authors gratefully acknowledge Prof. D. Buttrey, University of Delaware, for providing the K-free bismuth molybdate single-crystal materials.



Supporting information for this article is available on the WWW under <http://dx.doi.org/10.1002/anie.201001804>.

Figure 2: ZrV_2O_7 and a $\text{V}_2\text{O}_5/\text{ZrO}_2$ catalyst of near-monolayer surface VO_x coverage are shown in Figure 1, and $\text{Ce}_8\text{Mo}_{12}\text{O}_{49}$ and $\text{MoO}_3/\text{CeO}_2$ (Mo content ca. 80% of theoretical MoO_x monolayer capacity) are shown in Figure 2. In all cases, the initial V and Mo signals were strong whereas the initial counterion signals were low and increased as the surface was sputtered by the He ions (Figure 1a, 2a are from bulk phases, Figure 1c, and 2c are from supported systems). The Zr/V and Ce/Mo intensity ratios extrapolate to very small values at zero sputtering time for the bulk phases (Figure 1b, 2b) which reflects surface enrichment by V and Mo, respectively. In the supported $\text{V}_2\text{O}_5/\text{ZrO}_2$ catalyst, Zr was not initially exposed (Figure 1d, cf.

Ref. [19]) whereas for the submonolayer $\text{MoO}_3/\text{CeO}_2$ catalyst a finite initial Ce/Mo ratio was found (Figure 2d), that was much larger than for the bulk molybdate (Figure 2b). Diverging trends can be seen only at longer sputter times: For the Zr/V mixed oxides, the Zr/V intensity ratio leveled off for bulk ZrV_2O_7 but went on increasing for the supported $\text{V}_2\text{O}_5/\text{ZrO}_2$ catalyst. The difference arises from the underlying compositions uncovered by the sputter process. The asymptotic behavior seen with bulk ZrV_2O_7 (Figure 1b) is due to the presence of V in the bulk phase whereas the increasing Zr/V ratio in the supported system, Figure 1c,d, is related to the absence of V in the ZrO_2 support. With the Ce/Mo mixed oxides, the trends are similar in the LEIS spectra though their reflection in the numerical Ce/Mo ratios is less clear (Figure 2).

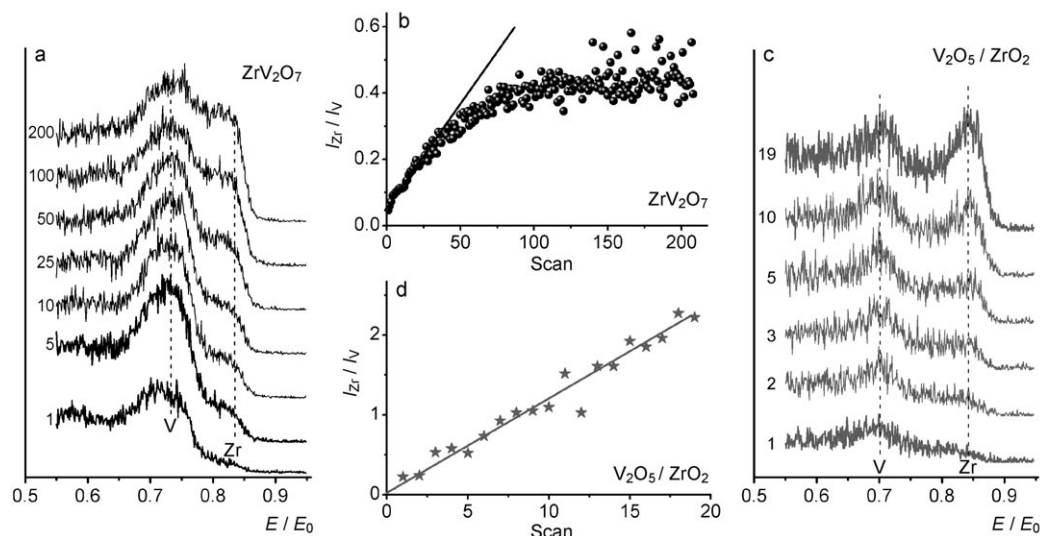


Figure 1. LEIS sputter series and intensity trends measured with Zr/V mixed oxides. a),b) ZrV_2O_7 , $E_0=1000$ eV, c),d) 4 wt% $\text{V}_2\text{O}_5/\text{ZrO}_2$ (V content (7.5 atoms per nm^2) near the theoretical monolayer limit, see Table S1 in the Supporting Information), $E_0=1000$ eV.

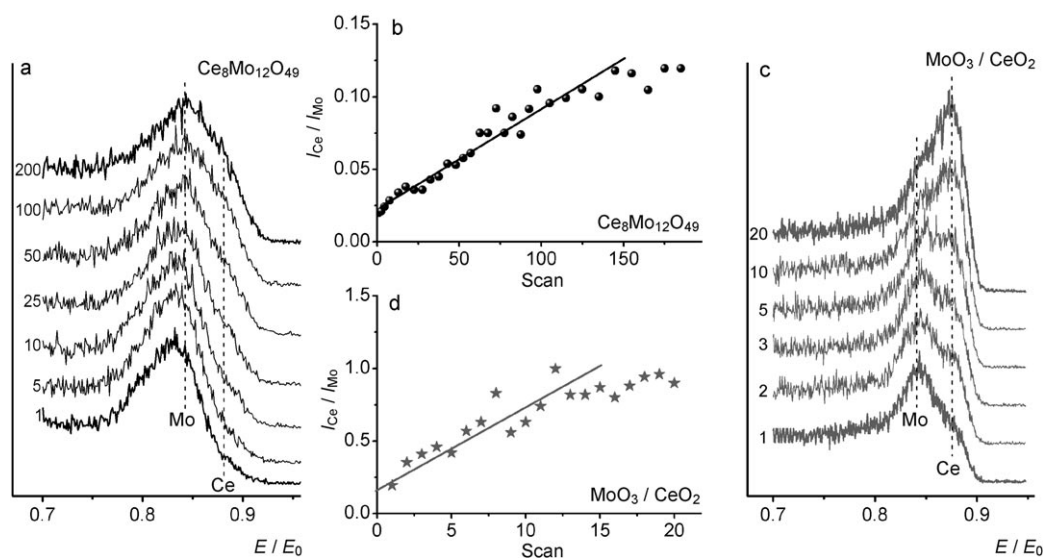


Figure 2. LEIS sputter series and intensity trends measured with Ce/Mo mixed oxides. a),b) $\text{Ce}_8\text{Mo}_{12}\text{O}_{49}$, $E_0=1000$ eV, c),d) 2.7 wt% $\text{MoO}_3/\text{CeO}_2$ (Mo content (3.6 atoms per nm^2) ca. 80% of the theoretical monolayer limit, cf. Table S1 in the Supporting information), $E_0=2000$ eV.

reflection in the numerical Ce/Mo ratios is less clear (Figure 2).

Conventional XPS did not detect any surface V enrichment for ZrV_2O_7 (Table 1). Some surface Mo enrichment was found for $\text{Ce}_8\text{Mo}_{12}\text{O}_{49}$, but a comparison of the initial LEIS intensity ratios in Figures 2b and 2d suggests that the Ce exposure in the external surface layer of $\text{Ce}_8\text{Mo}_{12}\text{O}_{49}$ was probably much smaller than indicated by the XPS result.

XPS spectra of bulk ZrV_2O_7 recorded with different excitation energies (ERXPS) are presented in Figure 3a. The plot of P (the V 3p/Zr 4p intensity ratio) versus the excitation energy (E_0 ; Figure 3b) was modeled with a variety of concentration depth profile functions (see examples in Figure 3c). Except for some physically meaningless versions, all models providing acceptable fits (Figure 3b) involved a dense, thin surface layer of exclusively vanadium oxide species. In the one shown, a 0.6 nm thin VO_x layer covers

Table 1: Bulk mixed oxides studied: Preparation routes and conventional XPS analysis.

Oxide	Metal	Preparation route ^[a]	XPS lines used	Mo/M or V/M ratio	
ZrV ₂ O ₇	Zr	A	V 2p _{3/2} , Zr 3d	2	bulk XPS ^[b] 2.0
AlVO ₄	Al	A	V 2p _{3/2} , Al 2p	1	0.63
Fe ₂ (MoO ₄) ₃	Fe	B	Mo 3d, Fe 2p	1.5	1.83
CoMoO ₄	Co	B	Mo 3d, Co 2p	1	0.93
NiMoO ₄	Ni	B	Mo 3d, Ni 2p	1	0.94
MnMoO ₄	Mn	B	Mo 3d, Mn 2p	1	0.84
Ce ₈ Mo ₁₂ O ₄₉	Ce	B	Mo 3d, Ce 3d	1.5	2.5
α-Bi ₂ Mo ₃ O ₁₂ (K)	Bi	C	Mo 3d, Bi 4f	1.5	1.72 (K:Bi=0.09)
γ(H)-Bi ₂ MoO ₆ (K)	Bi	C	Mo 3d, Bi 4f	0.5	0.33 (K:Bi=0.10)
α-Bi ₂ Mo ₃ O ₁₂	Bi	D	Mo 3d, Bi 4f	1.5	1.08
γ(H)-Bi ₂ MoO ₆	Bi	D	Mo 3d, Bi 4f	0.5	0.86

[a] A: citrate-based route, from NH₄VO₃ and metal nitrates;^[12,14] B: coprecipitation, from (NH₄)₆Mo₇O₂₄·4H₂O and metal nitrates; C: solid-state reaction between α-Bi₂O₃ and MoO₃;^[26] D: purified phases, see Supporting Information. [b] Photoionization cross sections from Ref. [27] used together with an empirical correction for dependence of spectrometer sensitivity of the kinetic energy of the photoelectrons.

another layer that still has some V enrichment (ca. 80% V, 1.3 nm thick) before the composition decays to the (fixed) bulk value of 67% V. The significance of the intermediate layer may be doubtful, but it may reflect a smooth transition from the enriched surface layer to the bulk composition. Models with single surface layers and free bulk concentration reproduced the data only at the expense of a significantly

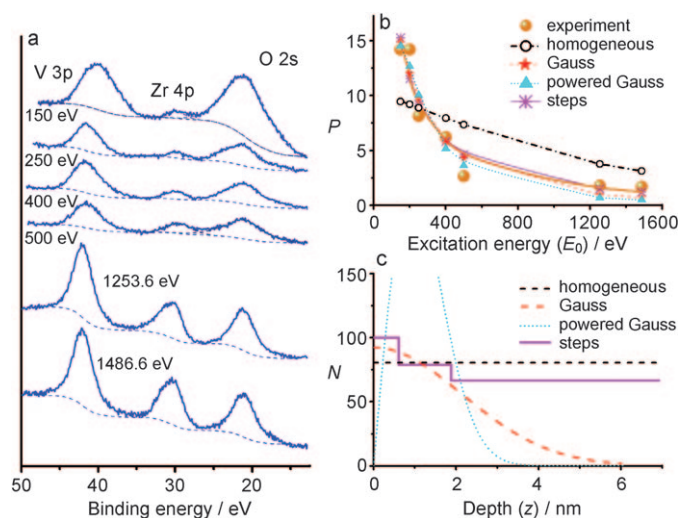


Figure 3. ERXPS analysis of the ZrV₂O₇ surface. a) spectra taken at different excitation energies (intensities scaled with different factors for representation in a single Figure, BE scale referenced to O 2s orbitals = 21.0 eV, see Supporting Information), b) dependence of experimental intensity ratios on excitation energies, modeled on the basis of different mathematical concentration depth profile types (see (c)), c) Optimized depth-profile functions ($N = 100 \times$ the number of V atoms divided by the sum of the V and Zr atoms). Note that the Gauss and powered Gauss results are unrealistic towards the bulk of the material. Due to unspecified influences of surface roughness, the actual thickness of the layer(s) may be smaller, see text.

depleted V content below the surface. Notably, ERXPS overestimates the depth coordinate below rough surfaces,^[20] therefore, the 0.6 nm thickness of the VO_x overlayer is rather an upper limit. As the extent of overestimation is on the order of 20–60%, except for roughness profiles with many clefts,^[20] the actual thickness of this overlayer is probably 0.3–0.4 nm. This value supports the view that stoichiometric ZrV₂O₇ is terminated by a monomolecular surface VO_x layer.^[14]

More examples of stoichiometric bulk mixed oxides strongly enriched with surface VO_x or MoO_x species are given in the Supporting Information: AlVO₄ compared with a model V₂O₅/Al₂O₃ catalyst (Figure S1: LEIS), NiMoO₄ (Figure S2: LEIS), and Fe₂(MoO₄)₃ (Figure S3a,b: LEIS,

Figure S3c,d: ERXPS). For the Fe₂(MoO₄)₃, the best ERXPS model fit suggests a 0.35 nm overlayer of exclusively Mo oxide species on an extended subsurface phase still enriched in Mo relative to the bulk (Figure S3c,d). From a recent STEM study, House et al. reported a near-surface 5–8 nm Mo enrichment zone in Fe₂(MoO₄)₃ crystals.^[21] According to our results, this zone supports an outermost layer containing almost exclusively Mo oxide species. Conventional XPS data (Table 1) are in disagreement with these findings for NiMoO₄ and AlVO₄ while a Mo surface enrichment found for Fe₂(MoO₄)₃ seems to track the thicker Mo enrichment zone found by House et al.^[21]

Some examples that prevent the tempting generalization that the surfaces of all stoichiometric bulk molybdates or vanadates are more or less completely covered by a Mo or V oxide overlayer are given in Figure 4 and Figure S4 in the Supporting Information. Neither with CoMoO₄ nor with MnMoO₄ is there any significant change of the signal shapes

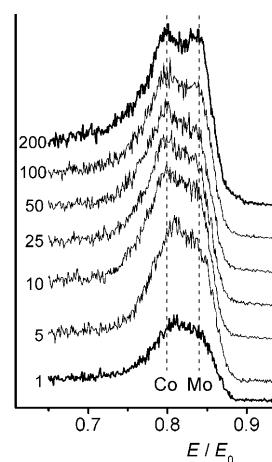


Figure 4. LEIS sputter series of bulk CoMoO₄, E₀ = 1000 eV.

along the LEIS sputter series: Apparently, their surfaces had the same compositions as the subsequent layers, which may still deviate from the bulk compositions. Conventional XPS indicated a slight Mo depletion in the external surface region for both compounds (Table 1).

Trace impurities in the bulk phase that segregate to the oxide surface are known to influence surface properties.^[22] We have experienced this with bismuth molybdate phases, which are ingredients of industrial propene (amm)oxidation catalysts.^[4,5] The LEIS measurements of phases containing potassium originating either from crucible walls or from commercial precursor compounds, and of samples purified by recrystallization procedures utilizing zone refinement effects are shown in Figure 5 and Figures S5–S7 in the Supporting Information. The alkali-metal-contaminated surfaces are of practical relevance as commercial bismuth molybdate catalysts are mostly promoted by alkali-metal ions.^[23,24]

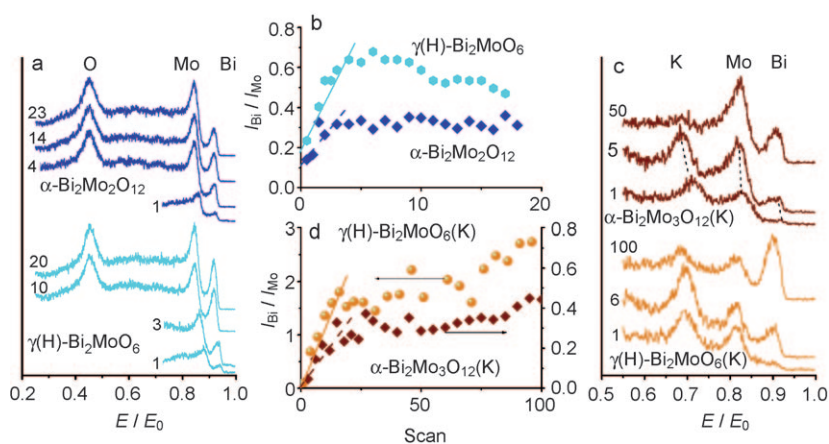


Figure 5. LEIS sputter series of pure and potassium-contaminated bulk bismuth molybdates. a) pure $\gamma(\text{H})\text{-Bi}_2\text{MoO}_6$ and $\alpha\text{-Bi}_2\text{Mo}_3\text{O}_{12}$, $E_0 = 2000$ eV, b) Bi/Mo intensity trends related to a, short scans accounted for according to scan duration, c) K-containing $\gamma(\text{H})\text{-Bi}_2\text{MoO}_6(\text{K})$ and $\alpha\text{-Bi}_2\text{Mo}_3\text{O}_{12}(\text{K})$, $E_0 = 1000$ eV, d) intensity trends related to (c). For K/Mo intensity trends see Supporting Information, Figure S6b,c.

In the pure phases (Figure 5a, Figure S7 in the Supporting Information), a clear Bi signal was already present in the first scan. After a short initial increase, the Bi/Mo intensity ratios leveled off or decayed ($\gamma(\text{H})\text{-Bi}_2\text{MoO}_6$, see also $\alpha\text{-Bi}_2\text{Mo}_3\text{O}_{12}$, Figure S7 in the Supporting Information). With potassium present (Figure 5c,d, and Figures S5, S6 in the Supporting Information), the Bi signal was initially very small and grew significantly upon sputtering. The Bi/Mo intensity ratios extrapolated to zero for $t=0$ (Figure 5d) except for phases with large Bi excess (Figure S5, S6 in the Supporting Information). The strong potassium signal decreased upon sputtering without disappearing completely (Figure 5, and Figure S5, S6 in the Supporting Information). The dramatic surface Mo enrichment of potassium-containing bismuth molybdates was not found by conventional XPS (Tables 1, Figure S2 in the Supporting Information): The data do not correlate with either the surface Mo enrichment or depletion that is suggested by LEIS for the potassium-containing and for the pure phases.

The present study of stoichiometric bulk mixed molybdate and vanadates suggests that their outermost surface layers may be strongly enriched or almost completely covered with MoO_x and VO_x species. This enrichment region is probably limited to approximately one atomic layer according to the ERXPS measurements, which makes the outermost surface resemble that of the corresponding model supported metal oxide catalyst. The enrichment is a result of surface reconstruction rather than preferential exposure. Even if truncation of bulk mixed-oxide structures was preferentially exposing one of the component elements at the surface, this would not give the net concentration gradient normal to the surface as detected in this study.

As seen in the study with bismuth molybdate phases, alkali-metal contamination may cause such surface reconstruction. Competition between potassium and surface BiO_x in their interaction with the molybdate appears to result in outer surfaces primarily constituted of surface MoO_x and KO_x species. Re-inspection or re-measurement of the LEIS spectra of all the remaining samples demonstrated that their surfaces were not contaminated by any alkali-metal or alkaline-earth metal ions that could be differentiated from the other elements by LEIS, except for AlVO_4 , where minor surface potassium concentrations would be difficult to detect between the Al and V signals. The observed surface enrichment might be explained by differences in free surface energies. These energies are lower for V=O and Mo=O terminated surface VO_x or MoO_x species than for the metal-OH terminated species of the counterions.^[25] However it seems to be too early to make any generalizations because of the lack of surface enrichment found for Co and Mn molybdate.

The data reported herein sound a note of caution regarding the discussion of catalytic reaction mechanisms on the basis of surface structures obtained by the truncation of the bulk mixed-oxide structure. Apparently, surface reconstruction is a frequent phenomenon and can be present even in the initial calcined stoichiometric mixed-metal oxides. Additional reconstruction of such overlayers may take place during catalysis (e.g. in selective hydrocarbon oxidations as suggested by synchrotron-based in situ XPS studies^[10]). Thus, more sophisticated surface analysis work is clearly needed to develop realistic reaction mechanisms for bulk mixed-metal oxide catalysts. The present study confirms that conventional XPS is of limited value for this analysis, although its failure to detect the enrichment phenomena seen by LEIS and ERXPS indeed confirms that these phenomena are confined to the outermost surface layer(s). Still, conventional XPS gives valuable information about deeper-lying enrichment or depletion zones as suggested by the results with $\text{Fe}_2(\text{MoO}_4)_3$ (Table 1, Figure S3c,d in the Supporting information). As to the outermost surface layer, further progress will mainly rely on synchrotron-based XPS as it can be used in situ, unlike LEIS.

Quantitative assessment of depth composition profiles inherent in the synchrotron-based XPS intensity data as exemplified in this study (ERXPS) may become a useful complement to the new synchrotron-based in situ XPS techniques.

Experimental Section

Sample preparation routes and results of conventional XPS analysis are summarized in Table 1. More detailed information on supported catalysts, other bismuth molybdate phases, phase identification, etc. is given in the Supporting Information. LEIS and conventional XPS spectra were measured with a Leybold surface analysis system equipped with an EA 10/100 MCD electron (ion) analyzer (Specs). Synchrotron XPS was measured at the HESGM beamline of BESSY-II (Berlin). For a description of ERXPS analysis see Ref. [20] and the Supporting Information.

Received: March 26, 2010

Revised: July 9, 2010

Published online: September 15, 2010

Keywords: LEIS · mixed oxides · molybdates · surface composition · vanadates

-
- [1] R. M. Cannon, *Ceram. Trans.* **2000**, *118*, 427.
 [2] J. Luo, *Crit. Rev. Solid State Mater. Sci.* **2007**, *32*, 67.
 [3] A. Avishai, C. Scheu, W. D. Kaplan, *Acta Mater.* **2005**, *53*, 1559.
 [4] R. K. Grasselli, J. D. Burrington, in *Handbook of Heterogeneous Catalysis, Vol. 7*, 2nd ed. (Eds.: G. Ertl, H. Knözinger, F. Schüth, J. Weitkamp), Wiley-VCH, Weinheim, **2008**, p. 3479.
 [5] R. K. Grasselli, A. A. Tenhover, in *Handbook of Heterogeneous Catalysis, Vol. 7*, 2nd ed. (Eds.: G. Ertl, H. Knözinger, F. Schüth, J. Weitkamp), Wiley-VCH, Weinheim, **2008**, p. 3489.
 [6] R. K. Grasselli, *Catal. Today* **2005**, *99*, 23.
 [7] B. Pawelec in *Metal Oxides—Chemistry and Applications* (Ed.: J. L. G. Fierro), CRC Francis & Taylor, Boca Raton, **2006**, p. 111.
 [8] N. Erdman, K. R. Poepplmeier, M. Asta, O. Warschkow, D. E. Ellis, L. D. Marks, *Nature* **2002**, *419*, 55.
 [9] V. V. Gulians, J. B. Benzinger, S. Sundaresan, N. Yao, I. E. Wachs, *Catal. Lett.* **1995**, *32*, 379.
 [10] H. Bluhm, M. Hävecker, E. Kleimenov, A. Knop-Gericke, A. Liskowski, R. Schlögl, D. S. Su, *Top. Catal.* **2003**, *23*, 99.
 [11] H. H. Brongersma, M. Draxler, M. de Ridder, P. Bauer, *Surf. Sci. Rep.* **2007**, *62*, 63.
 [12] L. E. Briand, A. H. Hirt, I. E. Wachs, *J. Catal.* **2001**, *202*, 268.
 [13] L. J. Burcham, L. E. Briand, I. E. Wachs, *Langmuir* **2001**, *17*, 6164.
 [14] L. E. Briand, J.-M. Jehng, L. Cornaglia, A. H. Hirt, I. E. Wachs, *Catal. Today* **2003**, *78*, 257.
 [15] K. Routray, L. E. Briand, I. E. Wachs, *J. Catal.* **2008**, *256*, 145.
 [16] I. E. Wachs, *Catal. Today* **1996**, *27*, 437.
 [17] M. A. Banières, I. E. Wachs, *J. Raman Spectrosc.* **2002**, *33*, 359.
 [18] L. E. Briand, O. P. Tkachenko, G. M. , I. E. Wachs, W. Grünert, *Surf. Interface Anal.* **2004**, *36*, 238.
 [19] L. E. Briand, O. P. Tkachenko, M. Guraya, X. Gao, I. E. Wachs, W. Grünert, *J. Phys. Chem. B* **2004**, *108*, 4823.
 [20] S. V. Merzlikin, N. N. Tolkachev, T. Strunskus, G. Witte, T. Glogowski, C. Wöll, W. Grünert, *Surf. Sci.* **2008**, *602*, 755.
 [21] M. P. House, M. D. Shannon, M. Bowker, *Catal. Lett.* **2008**, *122*, 210.
 [22] G. Deo, F. D. Hardcastle, M. Richards, A. M. Hirt, I. E. Wachs, *ACS Symp. Ser.* **1990**, *437*, 317.
 [23] Y. Moro-Oka, W. Ueda, *Adv. Catal.* **1994**, *40*, 233.
 [24] N. X. Song, C. Rhodes, J. K. Bartley, S. H. Taylor, D. Chadwick, G. J. Hutchings, *J. Catal.* **2005**, *236*, 282.
 [25] H.-P. Boehm, H. Knözinger in *Catalysis—Science and Technology, Vol. 4* (Eds.: J. R. Anderson, M. Boudart), Springer, Berlin, **1983**, p. 39.
 [26] D. J. Buttrey, D. A. Jefferson, J. M. Thomas, *Philos. Mag. A* **1986**, *53*, 897.
 [27] J. J. Yeh, I. Lindau, *At. Data Nucl. Data Tables* **1985**, *32*, 1.
-